https://doi.org/10.17221/138/2018-SWR

The use of simple hydrological models to assess outflow of two green roofs systems

Vojtěch Skala[1], Michal Dohnal[1], Jana Votrubová[1], Vladimíra Jelínková[2]*

[1]Faculty of Civil Engineering, Czech Technical University in Prague, Prague, Czech Republic
[2]University Centre for Energy Efficient Buildings, Czech Technical University in Prague, Buštěhrad, Czech Republic

**Corresponding author: michal.dohnal@cvut.cz*

Citation: Skala V., Dohnal M., Votrubová J., Jelínková V. (2019): The use of simple hydrological models to assess outflow of two green roofs systems. Soil & Water Res., 14: 94–103.

Abstract: Hydrological response of anthropogenic soil systems, including green roofs, has crucial importance in many fields of water engineering and management. As a consequence, there is an increasing need for modelling of the anthropogenic soil systems behaviour. To obtain empirical data, two green roof test beds were established on a green roof of University Centre for Energy Efficient Buildings, Czech Technical University in Prague. Each test bed is 1 m^2 in area and is instrumented for the runoff monitoring. One test bed was filled with less permeable local soil, the other with highly permeable commercial soil substrate, both were planted with stonecrops. Two simple deterministic lumped models – a nonlinear reservoir model and a linear reservoir cascade model – were used to assess the hydrological response of these green roof systems. The nonlinear reservoir model seems more appropriate for extensive green roof systems than the linear reservoir cascade model because of better description of rapid system reaction typical for thin soil systems. Linear reservoir cascade model frequently failed to mimic internal variability of observed hydrographs. In systems with high potential retention (represented by the test bed with local soil), episodically applied models that consider the same initial retention capacity for all episodes do not allow plausible evaluation of the actual episode-related retention. In such case, simulation model accounting for evapotranspiration between the rainfall events is needed.

Keywords: extensive green roof; herbaceous perennials; linear reservoir cascade; nonlinear reservoir model; rainfall--runoff event; storm water detention

Increasing use of buildings with green roofs has various positive impacts in urbanized areas. The most important environmental benefits of green roofs are a decrease of storm event runoff and a delay of peakflow. These facts lead to a reduction of risk induced by sewer system overloading. Green roofs also contribute to the improvement of microclimate as the vegetation captures dust, cools the air, reduces noise, etc. On the other hand, the climate is a main external forcing the green roofs are subjected to (Stovin *et al.* 2012). The functioning of the green roofs is mostly given by soil substrate, drainage board (layers with the highest retention capacity and room for root growth) and vegetation (due to interception and transpiration). Vegetation has to be continuously monitored to verify its health state (Piro *et al.* 2017) and possible effects of ageing on green roof hydrological performance (De-Ville *et al.* 2018).

Evaluation of green roofs hydrological response needs high-quality data and adequate simulation models. These models may assist in effective designing of green roofs in various constructional and

Supported by the Czech Science Foundation, Project No. 17-21011S and by the Grant Agency of the Czech Technical University in Prague, Grant No. SGS18/171/OHK1/3T/11.

https://doi.org/10.17221/138/2018-SWR

climatic conditions (e.g., Brunetti *et al.* 2018). In general, either simple conceptual models or complex soil-hydrology models solving Richard's equation are applicable for runoff prediction from green roofs. Conceptual models are computationally less intensive and have easily interpretable parameters (Locatelli *et al.* 2014). For example, Palla *et al.* (2012) compared the performance of simple conceptual model (similar to the model used by Stovin *et al.* (2012)) and complex soil-hydrology model adapted for the green roof (e.g., typical green roof vertical profile simulated by Hydrus-1D). They found the complex model more accurate but the conceptual model still applicable to green roof designing, especially when little information is available. However, results vary according to how the model is used (episodic vs. continuous basis) (Kasmin *et al.* 2010).

The main goal of the present study is to assess the adequacy of two simple hydrological models for predicting runoff from green roof systems. These models represent first-choice methods that can be easily implemented and could be treated as reference for other cases. The specific objectives are twofold: (1) to adapt two simple models, a nonlinear reservoir model and an linear reservoir cascade model, for modeling the hydrological response of two green roof test beds, and (2) to compare the model results against the experimental data in order to test the model applicability for modeling the hydrological behavior of green roof system.

MATERIAL AND METHODS

Experimental site. The experimental site is located on an extensive green roof of the University Centre for Energy Efficient Buildings, Czech Technical University In Prague, Czech Republic (coordinates 50°9.41797'N, 14°10.19195'E). The roof has an area of 941 m^2, a mean slope of 2%, and an elevation of 355 m above sea level or 10 m above the surrounding terrain. The area is characterized by a mild climate with the mean annual precipitation amount of 500 mm and the mean annual temperature of 8°C.

At the site, two green roof test beds with continuously measured outflow are installed (see next section for details). The site is also equipped for monitoring of the rainfall (rain gauge Young 52202-R.M. Young Company, 200 cm^2 catchment area, resolution 0.1 mm) the air and soil temperatures, the wind speed and direction, the air relative humidity and the net radiation. All hydrometeorological data are recorded with one-minute time step.

Test bed construction and instrumentation. The two green roof test beds, hereafter denoted by S1 and S2, were assembled in June 2014. Both test beds have identical structure. They have a metal construction insulated to prevent unwanted thermal influence, adjustable legs allowing variable slope (set to 2% in our study), and the catchment area of 1 m^2. The vertical profile (Figure 1) was as follows: vegetation cover (stonecrops), soil substrate (depth of 50 mm), filter textiles, a drainage layer (drainage board, Optigreen type FKD 25 W), protection textiles, a water-resistive layer, and thermal insulation (extruded polystyrene foam). Both test beds were equipped with tipping bucket flowmeters.

The only difference between the test beds is the type of the substrate used and the drainage board maximal retention capacity. S1 was filled with topsoil scraped at a nearby allotment with admixed light components (e.g., ceramsite and crushed bricks), referred to as Technosol (1.15 g/cm^3, total organic carbon in solid 2.30% C). The measured soil porosity is 0.54 cm^3/cm^3, the drainage board retention capacity is 5 mm. Hydraulic and thermal properties of Technosol type soils were studied by Kodešová *et al.* (2014). S2 was filled with a commercial lightweight substrate (Optigreen green roof extensive substrate Type E) consisting of expanded shale, lave, pumice, clay, crushed bricks, and green waste compost (0.77 g/cm^3, total organic

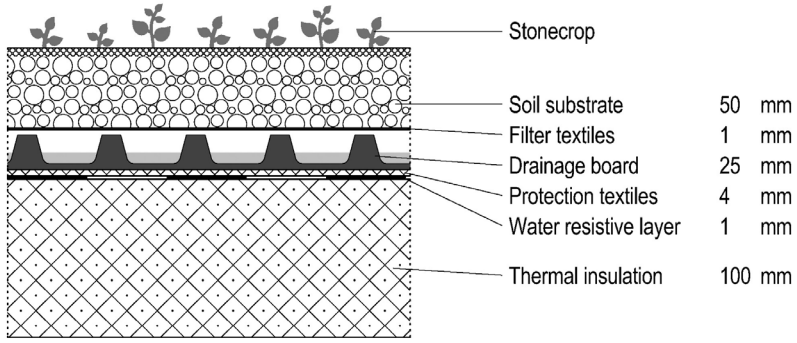

Figure 1. Vertical profile of the test beds

https://doi.org/10.17221/138/2018-SWR

carbon in solid 0.73% C). The measured soil porosity is 0.35 cm^3/cm^3, the drainage board retention capacity is 3.6 mm. Stonecrops were planted on the 9th of July 2014 in the test bed S1 and on the 4th of September 2014 in S2. The mixture of sedum (*Sedum album*, *Sedum hybridum*, *Sedum spurium*, *Sedum acre*) was used. The development of vegetation cover was regularly monitored (Jelínková *et al.* 2015).

Principally, the hydrological performance of a green roof during a rainfall consists of retention (i.e., reduction of the runoff volume) and detention (i.e., delay and redistribution of the runoff over time). Note that our test beds with an area of 1 m^2 are a representative substitute for green roofs regarding the retention function. The detention functioning expressed in the temporal redistribution of runoff is closely related to the size and geometry of the roof and thus the observed data are directly relevant only for very small roofs (i.e., with distance to the conduit less than 1 m). Larger green roofs will likely manifest more complex runoff reaction controlled mainly by the drainage layer functioning.

Experimental data. The rainfall and outflow from the test beds observed between September 2014 and November 2015 are used in the present study. The experimental data measured with one-minute time step were aggregated to five-minute time steps. Discrete rainfall events were separated from the data series. The start of a rainfall event was set to the first observed tip of the rain gauge and the end to the last tip of the rain gauge. The minimum dry interval between separate events was considered to be 6 hours. Only events with total rainfall amount higher than 6 mm were used in further processing. In total, eight events in 2014 (events No. 1–8 in Table 1) and ten events in 2015 (events No. 9–18 in Table 1) were obtained. Each rainfall event was paired with the induced outflow from the test beds and the basic rainfall-runoff characteristics were calculated (Table 1). None of the rainfall events had the return period longer than one year (according to Němec 1965). The event-based runoff coefficients were calculated as a fraction of the amount of runoff to the amount of precipitation received during the event.

Table 1. Basic parameters of the selected rainfall-runoff events

Event No.	Initial time	Rainfall depth† (mm)	Max. rainfall intensity (mm/h)	Rainfall-runoff episode duration (min)	Runoff coefficient‡ (–)	
					S1	S2
1	08/09/2014 15:05	6.6	32.4	870	0.04	0.56
2	11/09/2014 15:20	51.4	30.0	1700	0.65	0.76
3	21/09/2014 19:45	12.2	38.4	525	0.17	0.49
4	13/10/2014 23:00	14.4	12.0	685	0.09	0.71
5	15/10/2014 10:50	11.4	16.8	1720	0.41	0.94
6	21/10/2014 22:00	6.1	12.0	530	0.05	0.37
7	22/10/2014 11:15	6.1	2.4	1320	0.39	0.98#
8	18/11/2014 02:55	23.4	4.8	2230	0.30	0.97#
9	27/04/2015 19:15	17.3	30.0	1515	0.17	0.58
10	05/05/2015 21:30	10.4	6.0	895	0.05	0.49
11	08/06/2015 21:50	13.9	6.0	940	0.12	0.55
12	25/07/2015 05:35	6.0	30.0	315	0.02	0.31
13	16/08/2015 16:00	14.9	43.2	735	0.11	0.68
14	17/08/2015 07:15	34.9	8.4	2185	0.90	1.00#
15	07/10/2015 04:35	20.2	6.0	2045	0.33	0.80
16	14/10/2015 03:10	17.2	6.0	3320	0.88	1.00#
17	19/11/2015 16:35	13.2	19.2	895	0.29	0.66
18	29/11/2015 23:15	12.2	6.0	2200	0.77	0.76

†The total rainfall depth of all inspected events in 2014 and 2015 was 131.6 and 160.2 mm respectively; ‡the runoff coefficient relating amount of runoff to the amount of precipitation received for the rainfall-runoff event; #due to the short failure of the outflow monitoring mechanism in S2 during the intense parts of rainstorms 7, 8, 14, and 16, approximate values of the runoff coefficients are presented; S1, S2 – test beds

https://doi.org/10.17221/138/2018-SWR

Nonlinear reservoir model. First, the three-parameter nonlinear reservoir model (NR model) described by Kasmin *et al.* (2010) was used. The model combines a simple nonlinear reservoir model, which links the outflow from the system, Q, to the actual detention storage, S, with a simple effective rainfall separation procedure prescribing that the storage S starts filling after the retention capacity of the system, R_{NR}, is filled. The water storage at a time interval i is described with a balance equation

$$S_i = S_{i-1} + P_i - Q_i \quad (1)$$

where:

S_{i-1} – water storage in the previous time step (mm)

P_i – the effective rainfall during the actual time step (mm)

Q_i – test bed outflow depth during the actual time step (mm)

P is given by the observed rainfall pulses, Q is related to the storage:

$$Q_i = k_{NR} S_{i-1}^{n_{NR}} \quad (2)$$

where:

the left hand side expresses the outflow depth $Q_i = q_i \Delta t$

q_i – outflow flux density (mm/min)

n_{NR} – routing parameter (–)

k_{NR} – routing parameter (mm$^{(1-n_{NR})}$/min)

Δt – time step(min)

For n_{NR} = 1 the model reduces to the linear reservoir system

Linear reservoir cascade model. Alternatively, the test bed reaction to rainfall was approximated with a series of linear reservoirs. Similarly as for NR model, effective rainfall is derived by subtracting the retention capacity R_{LC} from the initial part of the rainfall. Nash (1957) derived an equation describing outflow from a series of linear reservoirs induced by an instantaneous input of a unit volume (linear reservoir cascade, LC):

$$u = \frac{1}{k_{LC}\,\Gamma(n_{LC})} e^{-t/k_{LC}} \left(\frac{t}{k_{LC}}\right)^{n_{LC}-1} \quad (3)$$

where:

u – outflow from the system (1/min)

k_{LC} – exponential decay constant describing reaction of separate reservoirs (min)

n_{LC} – represents the number of reservoirs (–)

$\Gamma(n_{LC}) = (n_{LC} - 1)!$ – gamma probability distribution function

t – time (min)

The reaction of the system to a series of rainfall pulses is calculated as a convolution of rainfall pulses and the transformation function described by (3):

$$q_i = \sum_{j=0}^{i} P_j u_{i-j} \quad (4)$$

where:

q_i – outflow flux density at the end of a time increment i (mm/min)

P_j – preceding incremental rainfall pulses (mm)

Model application. All calculations were conducted in a constant five-minute time step. Models were applied episodically considering the same initial retention capacity for all episodes. The retention capacity value reflects integrated retention of the soil substrate and the drainage board, as well as the water intercepted on the construction and vegetation.

Both models treat the retention in the same way (see above), they differ in the detention mechanism. In NR model, the runoff at any time is determined solely by the volume of water in the detention storage at that time. In LC model, the runoff at any time reflects the distribution of the previous rainfall. In principle, both models become the same if n_{NR} = 1 and n_{LC} = 1.

Surface runoff is not explicitly considered in either model. The assumption could be substantiated by high permeability of soil substrates used and the fact that no surface runoff was observed on the test beds during the experimental period.

Optimization procedure and performance measures. Optimal parameters of both models were determined considering two subsets of rainfall-runoff events observed in separate vegetation seasons (optimization scenario A, giving separate results for 2014 and 2015). Alternatively, optimization was performed for a complete set of rainfall-runoff events including both vegetation seasons (optimization scenario B).

The optimization was conducted using generalized reduced gradient nonlinear method (Fylstra *et al.* 1998). The objective function was composed of the sum of squared residuals between observed and calculated cumulative runoff. Parameter optimization was constrained as follows: n_{LC} is between 1 to 10 (if n_{LC} = 1 the model reduces to the linear reservoir model; more than ten reservoirs do not bring additional flexibility to optimization process); k_{LC} and k_{NR} are positive (required in Eq. (2) and (3)); n_{NR} is between 1 and 10 (if n_{NR} = 1 the model reduces to the linear reservoir model).

Initial parameters' values should be reasonably close to optimal values to ensure convergence of

https://doi.org/10.17221/138/2018-SWR

optimization procedure for the nonlinear problem. The choice of the initial estimate can considerably affect optimization results. However, for tested models and dataset used, the effect of different randomly selected initial estimates on optimized parameter values was negligible (Skala 2018). Thus, for each model a single set of initial parameter estimates was used. Selected initial parameter values are presented in Table 2. Parameters n_{NR} and k_{NR} were set to values recommended by Kasmin *et al.* (2010). For LC model, two reservoirs in cascade and 10 min as an initial value of parameter k_{LC} were used. Initial values of retention capacity were estimated from known maximum retention capacity of substrate and drainage board.

Model performance was assessed using root mean square error (RMSE)

$$\mathrm{RMSE} = \left[n^{-1} \sum_{i=1}^{n} \left(q_i^{sim} - q_i^{obs} \right)^2 \right]^{1/2} \quad (5)$$

where:

q^{sim} – model predicted value of the outflow

q^{obs} – observed value

i – time step

n – number of time steps

The measure is dependent on the scale of the numbers used and has a unit of the analyzed variable. Thus, no generally acceptable values exist, however in our case it allows comparing model performances in respective seasons. Another performance measure was Nash-Sutcliffe model efficiency (NSE, Nash & Sutcliffe 1970)

$$\mathrm{NSE} = 1 - \frac{\sum_{i=1}^{n} \left(q_i^{sim} - q_i^{obs} \right)^2}{\sum_{i=1}^{n} \left(\mu - q_i^{obs} \right)^2} \quad (6)$$

where:

μ – mean of the observed outflows

Table 2. Initial parameter values used in optimization

Model	Parameter	S1	S2
Nonlinear reservoir model (NR)	n_{NR} (–)	2	2
	k_{NR} (mm$^{(1-n_{NR})}$/min)	0.15	0.15
	R_{NR} (mm)	10	4
Linear reservoir cascade (LC)	n_{LC} (–)	2	2
	k_{LC} (min)	10.0	10.0
	R_{LC} (mm)	10	4

k_{NR} and k_{LC} are empirical routing parameters; the n_{NR} is an empirical parameter and n_{LC} is a number of linear reservoirs in series; R indicates retention capacity of the whole test bed system; S1, S2 – test beds

NSE criterion ranges from $-\infty$ to 1. NSE < 0 represents situation when observed mean μ is a better approximation than the model prediction. NSE = 1 indicates a perfect match.

The performance criteria were evaluated separately for each rainfall-runoff event.

RESULTS AND DISCUSSION

Outflow characteristics. Initially, an overall hydrological performance of the test beds was assessed with the runoff coefficients (expressing what portion of the precipitation leaves the system as the outflow over a considered time period). The seasonal runoff coefficient relating total amount of runoff to the total amount of precipitation received during a given period (from September to November in 2014, and from April to November in 2015), for S1 was 0.38 in 2014 and 0.28 in 2015. The seasonal runoff coefficient for S2 was 0.73 in 2014 and 0.46 in 2015. The event based runoff coefficients (Table 1) varied broadly from 0.04 to 0.9 for S1 and from 0.31 to 1.00 for S2. The difference between the two test beds is caused mainly by their different retention capacity. Considering the drainage board characteristics and measured porosity of the substrates, the maximum retention capacity is about 7.7 mm in S1 and about 5.35 mm in S2. Additionally, the test beds differ in the vegetation coverage which affects the runoff characteristics too.

Higher organic matter content in the substrate S1 probably contributed to the better development of vegetation cover (Jelínková *et al.* 2016). Figure 2 shows changes in the plant coverage in time and the relationship between the plant coverage and the 50-day runoff coefficients. The clear difference between the runoff coefficients observed in S1 and S2 is probably related to the structural differences as discussed above. However, a decreasing trend of the runoff coefficient with increasing vegetation coverage can be seen in each test bed separately. The mechanisms by which the vegetation helps to reduce the runoff include rainfall interception and retention capacity recovery due to plant water uptake.

The lag times, i.e., the delay between the maximum rainfall intensity and the peak flow, were in average 57 min for S1 and 56 min for S2 (with high standard deviations of 83 and 76 min respectively). Due to multiple peak character of analyzed rainfall-runoff episodes observed year-to-year changes of lag times were not conclusive either.

https://doi.org/10.17221/138/2018-SWR

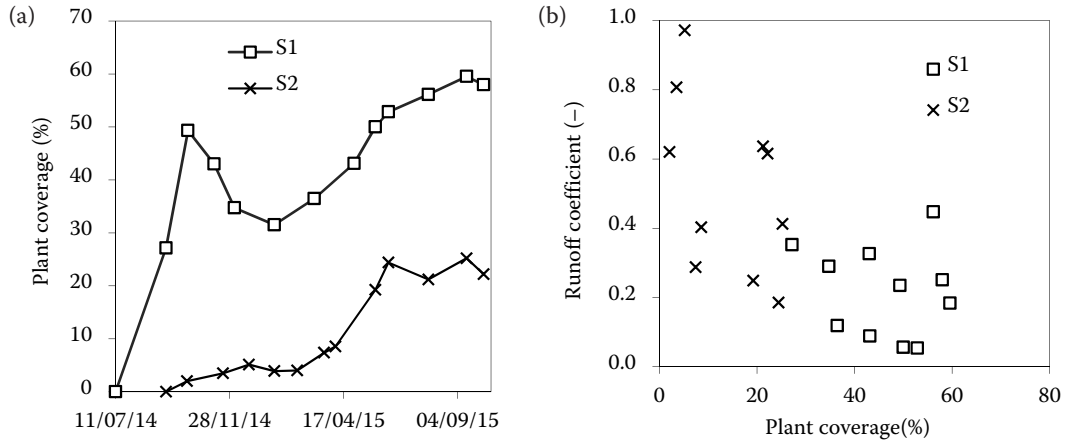

Figure 2. The development of the vegetation cover on both test beds (a) was monitored by a digital camera; each state of vegetation is compared with the runoff coefficient from the period covering 25 days before and after taking the picture (b); except two instances for which the continuous outflow record during the relevant 50-day period is not available

Effective parameter values – scenario A and B. First, parameters *k*, *n* and *R* were optimized to find an effective parameter set for each vegetation season (results for 2014 and 2015 presented in Table 3 and 4).

In case of test bed S1, both models described the runoff with acceptable values of RMSE, however, NSE criterion was negative in all instances. In general, the ability of both models to simulate measured data in test bed S1 was unsatisfactory, particularly regarding timing of runoff (negative values of NSE).

For test bed S2, both models provided acceptable results, NR model being more efficient in terms of both criteria (lower RMSE and higher NSE). Comparing model performance in separate seasons, the runoff in 2015 was simulated better in both test beds (see RMSE criterion in Table 3 and 4). This is probably due to the initial system settling and vegetation cover development occurring in 2014. The optimized integrated retention capacity of the roof system is lower than the initial guess (compare initial guess for S2 4 mm with optimized values 2.25 and 2.85 mm in average). This is an expected result as the initial value was estimated for an empty system while the optimized values reflect the fact that in some episodes the initial retention was partially depleted.

Note that for LC model, in three of the four cases the optimization reduced the reservoir cascade to a single linear reservoir. This is probably caused by fast reactions of analyzed green roof systems demonstrated by steep rising limbs of runoff hydrographs. It also indicates that the runoff at any time is mainly defined by the amount of water in detention storage without much influence from previous rainfall distribution.

Table 3. Effective parameter values of nonlinear reservoir (NR) model for scenarios A and B, i.e., optimization to rainfall--runoff events in both vegetation seasons and the whole dataset

Scenario	k_{NR} (mm$^{(1-n_{NR})}$/min)	n_{NR} (–)	R_{NR} (mm)	NSE (–)	RMSE (mm/h)
Test bed S1					
A (2014)	9.5E-01	1.8	14.9	–0.30 ± 0.42	0.75 ± 1.18
A (2015)	4.0E-06	6.1	5.7	–0.50 ± 0.88	0.46 ± 0.22
B (whole dataset)	4.0E-06	6.1	10.4	–0.03 ± 0.24	0.45 ± 0.36
Test bed S2					
A (2014)	4.7E-02	2.1	2.3	0.52 ± 0.25	0.82 ± 0.50
A (2015)	8.9E-03	3.6	2.2	0.66 ± 0.18	0.56 ± 0.24
B (whole dataset)	1.6E-02	3.1	2.2	0.59 ± 0.23	0.68 ± 0.41

NSE and RMSE values are arithmetic averages of criterions obtained for individual rainfall-runoff episodes included in the respective scenario and are complemented by standard deviations

https://doi.org/10.17221/138/2018-SWR

Table 4. Optimal parameter values of linear reservoir cascade (LC) model for scenarios A and B, i.e., optimization to rainfall-runoff events in both vegetation seasons and the whole dataset

Scenario	k_{LC} (min)	n_{LC} (–)	R_{LC} (mm)	NSE (–)	RMSE (mm/h)
Test bed S1					
A (2014)	10.5	1.0	10.2	–0.59 ± 1.72	0.51 ± 0.41
A (2015)	35.2	1.0	7.0	–1.39 ± 2.35	0.50 ± 0.20
B (whole dataset)	18.0	1.4	9.7	–1.24 ± 2.67	0.55 ± 0.42
Test bed S2					
A (2014)	34.8	1.0	1.7	0.48 ± 0.22	0.88 ± 0.55
A (2015)	7.3	2.2	4.0	0.48 ± 0.22	0.81 ± 0.62
B (whole dataset)	9.6	1.9	2.8	0.48 ± 0.21	0.84 ± 0.58

NSE and RMSE values are arithmetic averages of criterions obtained for individual rainfall-runoff episodes included in the respective scenario and are complemented by standard deviations

Characteristic performance of both models is illustrated in Figure 3 (results for rainfall-runoff event No. 13 for both test beds). In test bed S1, LC model provided better results than NR model. Particularly, the timing of the main runoff peak and the total runoff volume were satisfactorily described. On the other hand, the main peak flow was slightly overestimated and the first smaller peak was not captured. Regarding NR model results, neither timing nor shape of the simulated runoff corresponded to the measured data. The same rainfall-runoff episode in test bed S2 was correctly characterized by NR model. LC model provided an acceptable fit in term of volume. The internal variability of hydrograph, i.e., the falling limbs and the main peak, was poorly described.

Figure 3a illustrates a typical example of poorly described rainfall-runoff events with low runoff coefficient. In our case, it is associated with the model assumption that the system integrated retention capacity is the same for all rainfall-runoff events. In reality, it varies according to the previous history of rainfall and evapotranspiration. Consequently, the models fail to capture the runoff volume in individual rainfall-runoff events (see Figure 4 and related discussion). High potential retention capacity of the test bed S1 leads to a high variability in event-related actual retention and consequently to worse model predictions in terms of the event-related runoff volumes. High potential retention capacity causes the low runoff coefficients observed in test bed S1 compared with S2 (13 of 18 events have runoff coefficient lower than 0.35, see Table 1). The temporal variability of the effective retention capacity could be captured with continuous simulation accounting for evapotranspiration.

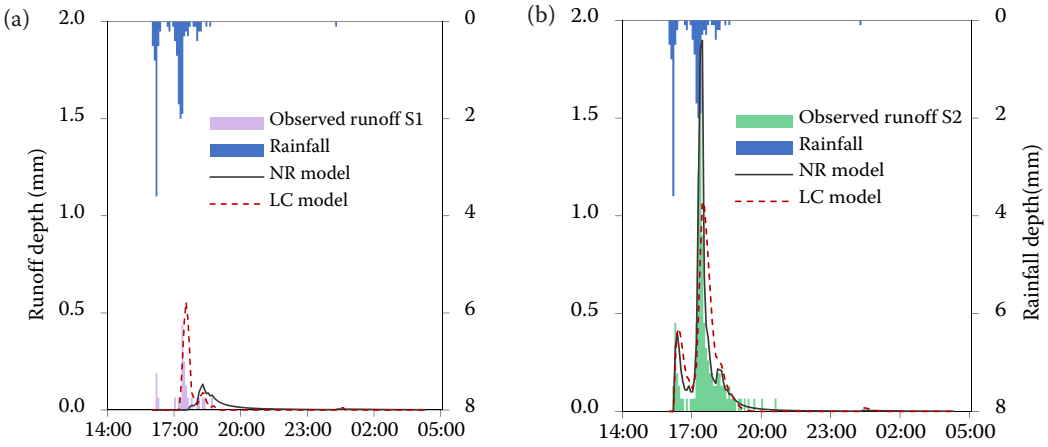

Figure 3. Example of nonlinear reservoir (NR) and linear reservoir cascade (LC) model performance for rainfall-runoff event No. 13 from 16th of August 2015 (results obtained with parameters optimized for individual years - scenario A); Nash-Sutcliffe model efficiency/RMSE value was –1.61/0.93 mm/h and –0.69/0.75 mm/h for NR and LC model respectively in S1 (a) and 0.88/1.17 mm/h and 0.49/2.44 mm/h for NR and LC model respectively in S2 (b)

https://doi.org/10.17221/138/2018-SWR

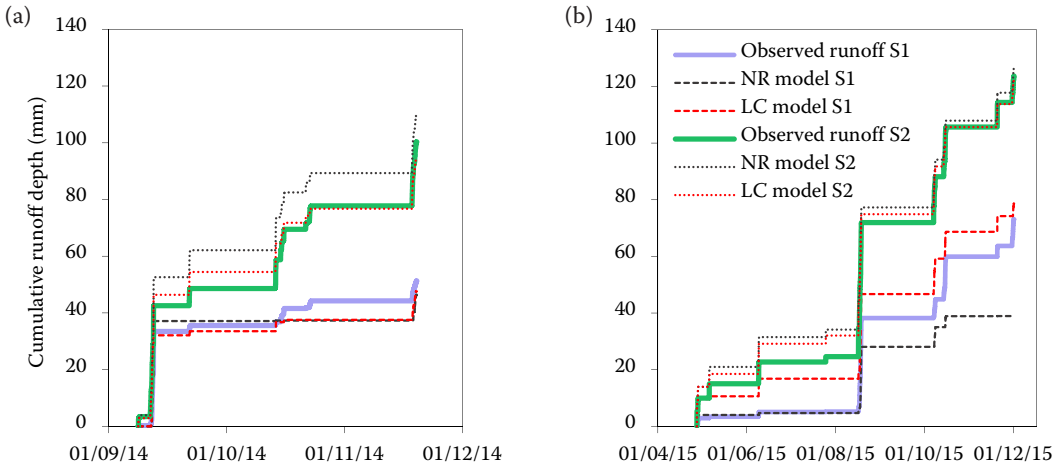

Figure 4. Comparison of measured and simulated runoff depth (results obtained with parameters optimized for individual years – scenario A) for nonlinear reservoir model (NR) and linear reservoir cascade model (LC); periods with measured data available in 2014 (a) and 2015 (b) are shown; only simulated rainfall-runoff event are included

Difficulty in capturing the low-runoff episodes is a more general problem. Krebs *et al.* (2016) dealt with a similar problem when modeling runoff from green roof test bed by SWMM LID-GR model. Their results suggest that the model performs better for events with higher runoff coefficients (e.g., > 0.50). Smaller rainfall-runoff events seem to be unsuitable for modeling with SWMM model. Krebs also figured out, that these events are not important for the determination of the total runoff because they produced less than 2% of the monitored runoff volume. However, in our case, events with the runoff coefficient below 0.35 acount for more then 20% of the total runoff volume. According to Krebs *et al.* (2016), to ensure better performance of the model for events with low runoff coefficients involving information about soil water status in the roof system is needed.

Figure 4 provides an overall comparison of simulated runoff volumes in scenario A. In 2014, measured and simulated total runoff depths were relatively close for both test beds (difference less than 10 mm for S2, and 5 mm for S1). In 2015, the fit of the total runoff is even better. The runoff volume estimation error on the episode basis is of the same extent (ex-

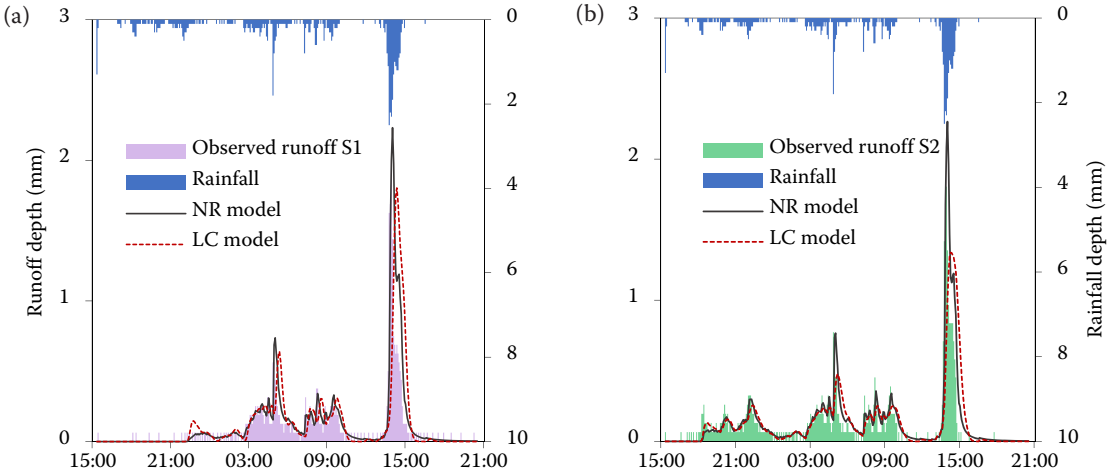

Figure 5. Example of nonlinear reservoir (NR) and linear reservoir cascade (LC) model performance for rainfall event No. 2 from September 11, 2014; individually evaluated Nash-Sutcliffe model efficiency/RMSE value of event No. 2 simulated by NR and LC model (Scenario B) in S1 was 0.57/1.69 mm/h and 0.45/1.91 mm/h, respectively (a); for S2 Nash-Sutcliffe model efficiency was 0.57/1.68 mm/h and 0.52/1.77 mm/h for NR and LC model, respectively (b)

https://doi.org/10.17221/138/2018-SWR

tremes are approximately ±10 mm). Better results are obtained for S2 compared to S1, and for 2015 compared to 2014. The inability of the models to describe the runoff volume is given by the assumption of a constant retention capacity for all episodes, as discussed above. It can be seen that for S1 in 2014 (Figure 4a), optimized NR model predicts no outflow in six of eight episodes. The worse simulation performance for S1 is given by higher variability of the episode-related retention capacity observed in S1 compared to S2 (calculated as the difference between the rainfall and runoff depths). On the other hand, very good simulation results were obtained for S2 in 2015 (coefficient of determination of cumulative runoff curves higher than 0.99).

Model parameters were alternatively optimized to determine parameters for the whole examined period. These effective parameter sets are in Tables 3 and 4.

In this scenario, both models provide acceptable results for test bed S2 only (NSE = 0.59 and 0.48). As expected, the results are slightly worse than the best in the previous scenario; optimization process was forced to find compromise value of parameters describing wider range of diverging situations. The performance of the models is presented on a well-described rainfall-runoff event No. 2 (Figure 5).

The difference in the total cumulative runoff depth between models and measured outflow (calculated for simulated episodes only) was less than 10%.

Comparison of the models' performance with parameter sets optimized either for the whole two-year period or separately for each season indicated low transferability of the results to other years or studies.

CONCLUSIONS

A nonlinear reservoir model and a linear reservoir cascade model were employed for modeling the runoff from experimental green roof test beds. The runoff was computed on episodic basis during major rainfall-runoff events in two consecutive vegetation seasons.

Comparing both models, the nonlinear reservoir model seems more appropriate for the extensive green roof systems than the linear reservoir cascade model. NR model provided better description of rapid system reaction, i.e., the steep rising limbs of hydrographs, typical for thin soil systems. The results may be affected by the small catchment area of the test beds.

For the test bed filled with the commercial substrate, NR model produces satisfactory results with RMSE below 0.82 mm/h and NSE above 0.52 in all optimization scenarios. LC model also yield acceptable results, however, in contrast with NR model, it frequently failed to mimic internal variability of observed hydrographs.

Neither model provided acceptable results for the test bed filled with locally prepared Technosol. This finding is related to higher maximum retention capacity of this test bed that causes higher variability of the episode-related actual retention capacity. Thus, the error introduced by assuming a constant retention capacity for all episodes is bigger in S1 than in S2. Moreover, as the higher retention capacity leads to lower overall runoff, the relative impact of this error becomes crucial.

In systems with higher potential retention, correct evaluation of episode-effective retention becomes crucial. Episodically applied models considering the same initial retention capacity for all episodes are not sufficient. Simulation models accounting for evapotranspiration between the rainfall events are needed.

Acknowledgments. Green roof system and meteorological data were available through the courtesy of the University Centre for Energy Efficient Buildings, Czech Technical University in Prague.

References

Brunetti G., Porti M., Piro P. (2018): Multi-level numerical and statistical analysis of the hygrothermal behavior of a non-vegetated green roof in a mediterranean climate. Applied Energy, 221: 204–219.

De-Ville S., Menon M., Jia X., Stovin V. (2018): A longitudinal microcosm study on the effects of ageing on potential green roof hydrological performance. Water, 10: 784–784.

Fylstra D., Lasdon L., Watson J., Waren A. (1998): Design and use of the microsoft excel solver. Journal Interfaces, 28: 29–55.

Jelínková V., Dohnal M., Picek T. (2015): A green roof segment for monitoring the hydrological and thermal behaviour of anthropogenic soil systems. Soil and Water Research, 10: 262–270.

Jelínková V., Dohnal M., Šácha J. (2016): Thermal and water regime studied in a thin soil layer of green roof systems at early stage of pedogenesis. Journal of Soils and Sediments, 16: 2568–2579.

Kasmin H., Stovin V., Hathway E.A. (2010): Towards a generic rainfall-runoff model for green roofs. Water Science and Technology, 62: 898–905.

https://doi.org/10.17221/138/2018-SWR

Kodešová R., Fér M., Klement A., Nikodem A., Teplá D., Neuberger P., Bureš P. (2014): Impact of various surface covers on water and thermal regime of Technosol. Journal of Hydrology, 519: 2272–2288.

Krebs G., Kuoppamaki K., Kokkonnen T., Koivusalo H. (2016): Simulation of green roof test bed runoff. Hydrological Processes, 30: 250–262.

Locatelli L., Mark O., Mikkelsen P.S., Arnbjerg-Nielsen K., Jensen M.B., Binning P.J. (2014): Modelling of green roof hydrological performance for urban drainage applications. Journal of Hydrology, 519: 3237–3248.

Nash J.E. (1957): The form of the instantaneous unit hydrograph. International Association of Hydrological Sciences General Assembly, 1957: 114–121.

Nash J.E., Sutcliffe J.V. (1970): River flow forecasting through conceptual models part I – a discussion of principles. Journal of Hydrology, 10: 282–290.

Němec J. (1965): Hydrology. Prague, State Publishing House of Technical Literature. (in Czech)

Palla A., Gnecco I., Lanza L.G. (2012): Compared performance of a conceptual and a mechanistic hydrologic models of a green roof. Hydrological Processes, 26: 73–84.

Piro P., Porti M., Veltri S., Lupo E., Moroni M. (2017): Hyperspectral monitoring of green roof vegetation health state in sub-mediterranean climate: preliminary results. Sensors, 17: 662.

Skala V. (2018): Modeling of runoff from green roof test beds. [Diploma Thesis.] Prague, Czech Technical University in Prague. (in Czech)

Stovin V., Vesuviano G., Kasim H. (2012): The hydrological performance of green roof test bed under UK climatic conditions. Journal of Hydrology, 414–415: 148–161.

Received for publication June 25, 2018
Accepted after corrections September 4, 2018
Published online January 11, 2019